An Empirical Characterization of Radio Signal Strength Variability in 3-D IEEE 802.15.4 Networks Using Monopole Antennas

Dimitrios Lymberopoulos, Quentin Lindsey, and Andreas Savvides

Embedded Networks and Applications Lab, ENALAB,
Yale Univerisity, New Haven, CT 06520, USA
{dimitrios.lymberopoulos, quentin.lindsey, andreas.savvides}@yale.edu,
abs@cs.yale.edu

Abstract. The wide availability of radio signal strength attenuation information on wireless radios has received considerable attention as a convenient means of deriving positioning information. Although some schemes have been shown to work in some scenarios, many agree that the robustness of such schemes can be easily compromised when low power IEEE 802.15.4 radios are used. Leveraging a recently installed sensor network testbed, we provide a detailed characterization of signal strength properties and link asymmetries for the CC2420 IEEE 802.15.4 compliant radio using a monopole antenna. To quantify the several factors of signal unpredictability due to the hardware, we have collected several thousands of measurements to study the antenna orientation and calibration effects. Our results show that the often overlooked antenna orientation effects are the dominant factor of the signal strength sensitivity, especially in the case of 3-D network deployments. This suggests that the antenna effects need to be carefully considered in signal strength schemes.

1 Introduction

The existence of radio connectivity and the attenuation of radio signal with distance are attractive properties that could potentially be exploited to estimate the positions of small-wireless devices featuring low-power radios. Radio signal strength indicator (RSSI), a standard feature in most radios, has attracted a lot of attention in the recent literature for obvious reasons. RSSI eliminates the need for additional hardware in small wireless devices, and exhibits favorable properties with respect to power consumption, size and cost. As a result, several RSSI based algorithms have been proposed that either assume a complete profiling of the network deployment area [1],[9][3],[15],[2],[8],[14],[16],[19] or a specific signal attenuation model that can provide distance or area information directly or indirectly from the raw RSSI data [21],[6],[7],[18],[11],[13],[12],[5].

Despite the increasing interest in signal strength localization using IEEE 802.14.5 radios, there is still a lack of detailed characterization of the fundamental factors contributing to large signal strength variability. To investigate these factors, and to get a better understanding of the asymmetries that arise in 3-D

K. Römer, H. Karl, and F. Mattern (Eds.): EWSN 2006, LNCS 3868, pp. 326–341, 2006.

schemarios, we present a detailed characterization of signal strength behaviors in an IEEE 802.15.4 sensor network with monopole antennas. Instead of proposing a specific algorithm, in this paper we focus on showing the sources of signal strength variability. We do so by collecting a large number of measurements from a 40-node testbed, both in an indoor and an open-field environment. This characterization differs from previous studies using IEEE 802.11 radios, since it examines a new radio technology with less powerful radio transmissions. Furthermore, a large fraction of the measurements are taken in a three-dimensional testbed deployment that emulates a realistic environment where sensor network deployments are likely to occur.

Our findings demonstrate that the relative antenna orientation between receiver-transmitter pairs is a major factor in signal strength variability, even in the absence of multipath effects. This suggests that many schemes using radio signal strength on similar radios should carefully consider these factors before going to actual deployments. The approximately 15,000 measurements collected for this study are available online at $http://www.eng.yale.edu/enalab/rssidata/$.

Our presentation of this paper proceeds as follows: Section 2 provides an overview of other characterizations and schemes that use signal strength. This is followed by a discussion of the signal strength variability components and a detailed evaluation of our system.

2 Related Work

Some of the issues related with received signal strength ranging where presented by Whitehouse et. al. in an outdoor scenario characterization described in [20].

Three recent sensor network localization algorithms using low power sensor node radios are Ecolocation [21], MoteTrack[9] and Probability Grid [18]. Ecolocation determines the location of unknown nodes by examining the ordered sequence of received signal strength measurements taken at multiple reference nodes. The key idea of Ecolocation is that the distance-based rank order of reference nodes constitutes a unique signature for different regions in the localization space. Ecolocation reports a location error of $10ft$ for a very small outdoor network deployment area ($26ft$ x $49ft$) while Probability Grid reports a location error that is equal to the 70%-80% of the communication range for a $410ftx410ft$ outdoor network deployment. In the case of Probability Grid it is assumed that the goal of the sensor network deployment is to form a grid topology. Given this a priori knowledge, Probability Grid attempts to compute in a probabilistic way the one-hop distance and the number of hops that an unknown node is far away from an anchor node. MoteTrack is very similar to RADAR[1] but it does not require a back-end server where all the data have to be transferred and processed. Conversely, in Moterack the location of each mobile node is computed using a received radio signal strength signature from numerous beacon nodes to a database of signatures that is replicated across the beacon nodes themselves. The location error reported by Motetrack is approximately $13ft$ for an indoor network deployment area of $18751ft^2$.

Several schemes have also been presented using IEEE 802.11 radios. In [6] a comparative study of many RSSI based localization techniques using 802.11 cards is presented. According to the results of this study all the localization techniques produce approximately the same location error over a range of environments.

Other work on RSSI-based localization algorithms has been developed in the context of two broad categories: map based such as [1],[9],[3],[15],[2],[8],[14],[16], [19], and distance (or area) prediction based [21],[6],[7],[18],[11],[13],[12],[5].

3 Experimental Infrastructure

In the next sections we quantify the sources of RSSI variability using our Zigbee based infrastructure. A three dimensional, battery operated scalable testbed in our lab is used for indoor sensor network deployments. The testbed illustrated in Figure 1(b) is a 3-D structure measuring 4.5m(W) x 6m(L) x 3m(H) and it is designed to host a large number of static and mobile nodes to instrument a variety of application scenarios. The centerpiece of our infrastructure is the XYZ sensor node [10], an open-source general purpose sensing platform designed around the OKI ML67Q500x ARM/THUMB microprocessor and the IEEE 802.15.4 compliant CC2420 radio from Chipcon [4].

The communication subsystem of the XYZ sensor node was designed so that the correct operation of the radio chip is ensured. The radio chip is powered by the on-board voltage regulator and thus fluctuations in the battery voltage level do not affect the operation of the communication subsystem. In addition, the area under the chip on the PCB is used for grounding and it is well connected to the ground plane with several vias. The ground pins of the radio are connected to ground as close as possible to the package pin using individual vias and the microcontroller (as well as its support circuitry) was placed far away from the radio chip in order to avoid interference with the RF circuitry.

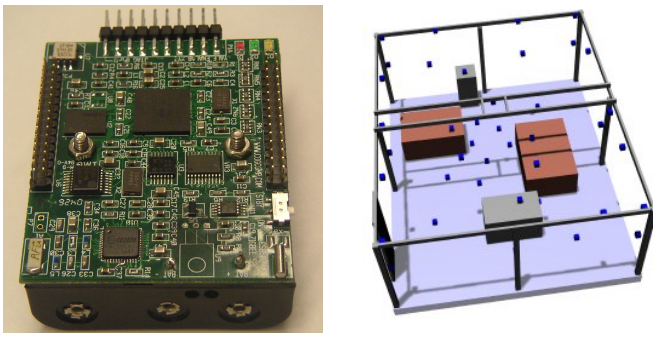

(a) (b)

Fig. 1. a) The XYZ sensor node, b) Testbed node placement

The Chipcon CC2420 IEEE 802.15.4 radio transceiver operates in the 2.4GHz ISM band and includes a digital direct sequence spread spectrum (DSSS) modem providing a spreading gain of $9dB$ and an effective data rate of $250Kbps$. It was specifically designed for low power wireless applications and supports 8 discrete power levels: $0dBm$, $-1dBm$, $-3dBm$, $-5dBm$, $-7dBm$, $-10dBm$, $-15dBm$ and $-25dBm$ at which its power consumption varies from $29mW$ to $52mW$[10]. A built-in received signal strength indicator gives an 8-bit digital value: $RSSI_{VAL}$. The $RSSI_{VAL}$ is always averaged over 8 symbol periods ($128\mu s$) and a status bit indicates when the $RSSI_{VAL}$ is valid (meaning that the receiver was enabled for at least 8 symbol periods). The power P at the RF pins can be obtained directly from $RSSI_{VAL}$ using the following equation:

$$P = RSSI_{VAL} + RSSI_{OFFSET}[dBm] \tag{1}$$

where the $RSSI_{OFFSET}$ is found empirically from the front-end gain and it is approximately equal to $-45dBm$. In the next sections when we refer to the RSSI value we refer to the $RSSI_{VAL}$ and not the power P unless otherwise stated.

A straight piece of wire is used as a monopole antenna for our sensor node. The length of our antenna is equal to $1.1inch$, the optimal antenna length according to the CC2420's datasheet [4]. In all of the experiments described in the next sections, the length of the antenna on all the nodes was $1.1inch$ unless otherwise stated.

4 Sources of RSSI Variability

In addition to multipath, fading and shadowing of the RF channel, signal strength measurements are also affected by the following factors:

1. **Transmitter variability:** Different transmitters behave differently even when they are configured exactly in the same way. In practice, this means that when a transmitter is configured to send packets at a power level of d dBm then the transmitter will send these packets at a power level that is very close to d dBm but not necessarily exactly equal to d dBm. This can alter the received signal strength indication and thus it can lead to inaccurate distance estimation.
2. **Receiver variability:** The sensitivity of the receivers across different radio chips is different. In practice, this means that the RSSI value recorded at different receivers can be different even when all the other parameters that affect the received signal strength are kept constant.
3. **Antenna orientation:** Each antenna has its own radiation pattern that is not uniform. In practice, this means that the RSSI value recorded at the receiver for a given pair of communicating nodes and for a given distance between them varies as the pairwise antenna orientations of the transmitter and the receiver are changed.

4.1 Path Loss Prediction Model

The majority of RSSI localization algorithms that do not use full location profiling of the deployment environment make use of a signal propagation model that maps RSSI values to distance estimates [17]. The most widely used signal propagation model is the log-normal shadowing model:

$$RSSI(d) = P_T - PL(d_0) - 10\eta \log_{10} \frac{d}{d_0} + X_\sigma \tag{2}$$

where, P_T is the transmit power, $PL(d_0)$ is the path loss for a reference distance d_0, η is the path loss exponent and X_σ is a gaussian random variable with zero mean and σ^2 variance, that models the random variation of the RSSI value.

Using the CC2420 radio we were able to verify the log-normal shadowing model in an obstacle-free environment(basketball court). The effects of orientation and calibration were isolated by taking measurements with a single pair of nodes, with the receiver and the transmitter on the same plane. Figure 5a shows the RSSI vs Distance plots. Based on our measurements in the basketball court, RSSI changes linearly with the log of the distance.

5 Variations Across Different Radios

In order to quantify the variability among different transmitter-receiver pairs we conducted 2 different experiments. To characterize transmitter variations we used a single receiver and 9 different transmitters. In all of our experiments the

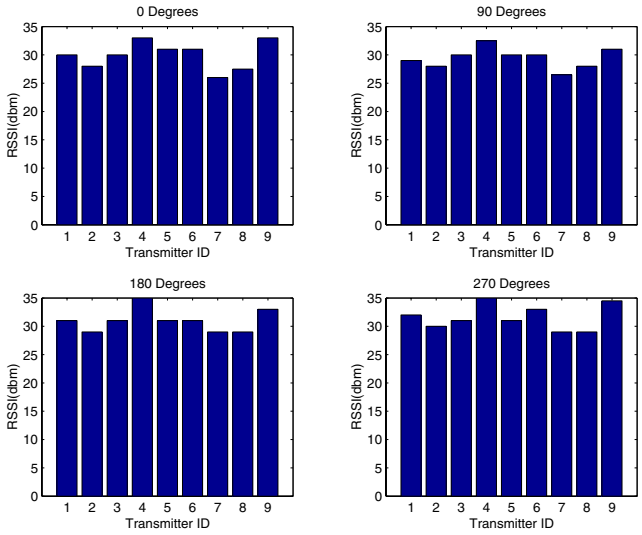

Fig. 2. Quantifying transmitter's variability

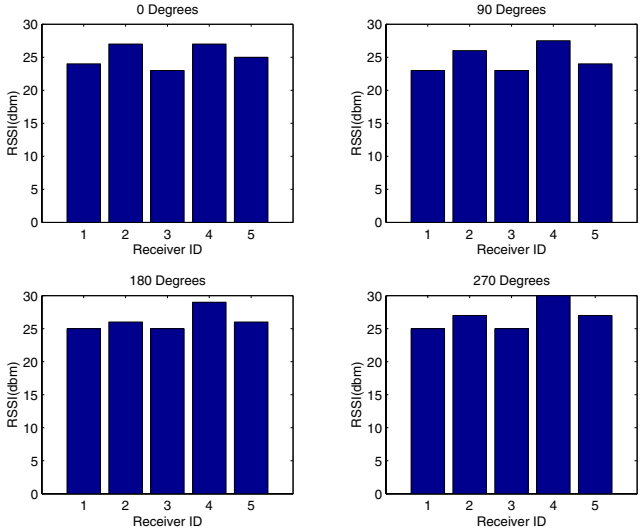

Fig. 3. Quantifying receiver's variability

receiver was exactly in the same position and with the same antenna orientation. One transmitter at a time was placed at a specific location that was $1.31ft$ far away from the receiver. Each transmitter was transmitting packets at $-15dBm$ while in 4 different orientations (0, 90, 180, and 270 degrees). The nodes under test were placed in the middle of a room without furniture in order to minimize the effect of the reflections in our measurements.

Figure 2 shows the RSSI values recorded at the receiver for all the transmitter and for all 4 orientations. For each orientation the average RSSI value and its standard deviation are computed. Averaging over all the average standard deviations for all different orientations we find that the overall standard deviation of the received RSSI value is equal to: $2.24dBm$. Using the log-normal signal propagation model shown in Figure 5a we find that the $2.24dBm$ RSSI standard deviation corresponds to $0.4ft$ distance standard deviation.

To quantify the variability in the receiver we used a similar setup using 1 transmitter and 5 different receivers. The transmitter was transmitting packets at $-15dBm$ while in 4 different orientations (0, 90, 180, and 270 degrees). Figure 3 shows the RSSI values recorded at the different receivers for all 4 orientations of the transmitter. For each orientation the average RSSI value and its standard deviation are computed. Averaging over all the average standard deviations for all different orientations we find that the overall standard deviation of the received RSSI value is equal to: $1.86dBm$. Using the log-normal signal propagation model shown in Figure 5a we find that the $1.86dBm$ RSSI standard deviation corresponds to $0.33ft$ distance standard deviation. The same experiment was performed several times with different transmitters in order to make sure that we were measuring the receiver variability and not something else that had to do with the specific transmitter.

6 Antenna Characterization

The XYZ sensor node, as most of the generic sensor node platforms, uses a simple wire as a monopole antenna. Ideally, the radiation pattern of this antenna should be uniform and it should look like a circle (2-D space) or a sphere (3-D space). Of course, this does not hold in practice. However, without knowing our antenna's radiation pattern it would be impossible to attempt inferring distance or location information directly from RSSI measurements.

We characterized our antenna in a basketball court measuring $79ft$ in length and $46ft$ in width. The ceiling of the court was at a height of $30ft$. In order to avoid the interference of the floor we attached our transmitter node to a string running from the one side of the court to the other. The transmitter node was at a height of approximately 8ft from the ground at the center of the court. Its antenna was vertical to the PCB board pointing down towards the floor.

We measured RSSI with a receiver node at 3 different heights from the floor: $1.25ft$, $3.5ft$, and $6.5ft$. For each one of these heights we measured the RSSI values for 8 different angles of the receiver with respect to the transmitter: 0, 45, 90, 135, 180, 215, 270, and 315 degrees. For each of these orientations we recorded the RSSI values on the receiver at a distance resolution of $2ft$. We stopped taking measurements for a given height and orientation only when the receiver was not able to receive any packets.

6.1 Antenna Length: Using a Suboptimal Antenna

According to the Chipcon's Zigbee radio chip datasheet [4] the optimal length of the monopole antenna should be 1.1inch. Therefore, in our first attempt to measure the antenna we used a wire with 1.1inch length as the monopole antenna. Both receiver and transmitter had exactly the same antenna.

Initially we tried to measure the antenna at the lowest power level ($-25dBm$) of the radio. We noticed that even at the lowest power level, transmitter and receiver could communicate for almost any position of the receiver in the basketball court. In addition, we noticed that the RSSI values recorded at the receiver were changing dramatically with very small changes in the distance between transmitter and receiver even when the orientation of the nodes was kept constant. Therefore, it was impossible to infer any signal propagation model based on the RSSI data. Apparently, even at the lowest power level the 802.15.4 radio from Chipcon has a large communication range that is able to generate significant reflections even in the basketball court. Hence, the results in a real indoor environment with furniture and people would be much worse. By increasing the transmission power level of the radio we found out that even at slightly higher power levels two nodes could communicate over long distances even without line-of-sight. To reduce the effective communication range of the nodes we used a suboptimal antenna. Instead of using the recommended length (1.1inch) monopole antenna we used a 2.9inch wire as our monopole antenna. As it can be seen in Figure 5b, the communication range of the radio when using the suboptimal antenna is significantly reduced but the signal attenuation properties remain the same.

6.2 Antenna Orientation in Basketball Court

After replacing the 1.1inch antennas, on both the receiver and the transmitter, with 2.9inch antennas we repeated the same experiment. At the lowest transmission power level of the radio the communication range was 3.3-6.6ft. Despite the fact that changing the length of the antenna reduced the communication range, still we could not get any signal propagation model at the lowest power level. It was obvious that communication was totally unreliable at the lowest power level with the 2.9inch antenna.

However, we noticed that by using the next higher transmission power level we were getting consistent RSSI values on the receiver and we had reliable communication in a wide range of distances. The same was valid for all the other transmission power levels. Therefore, we decided to measure the 2.9inch antenna at the power level of $-15dBm$ using all the possible combinations described in the previous section.

Figures 4a, 4b, and 4c show the RSSI values versus distance for all the orientations and for the $6.5ft$, $3.5ft$, and $1.25ft$ receiver heights respectively. Note that when the receiver is at $1.25ft$ (Figure 4c) and $3.5ft$ (Figure 4b) height from the ground the raw RSSI data cannot be used to infer any distance information. The reason is that significantly different distances can produce the same or almost the same RSSI values. In addition, similar distances correspond to very different (even up to $11dBm$) RSSI values for different antenna orientations.

However, when the receiver is at $6.5ft$ height from the ground (Figure 4a) the RSSI versus distance plot can be easily fitted to the widely used log-normal signal propagational model. Note that as the distance between transmitter and receiver increases the variability in the RSSI value that corresponds to this distance also increases. In other words different ranges of RSSI values provide distance information with different levels of accuracy. This suggests that a probabilistic approach for translating RSSI values to distance information should be used. This can be easily implemented by computing the probability distribution of the raw RSSI values over the different distances. Using this prob-

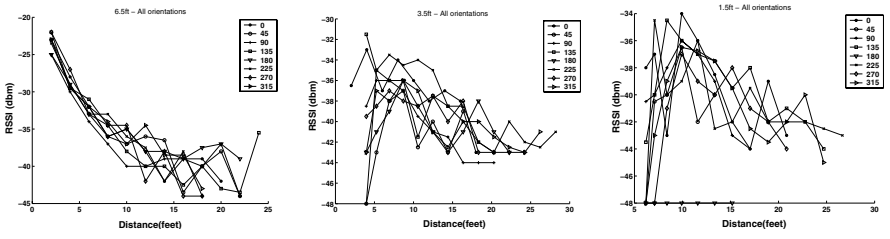

(a) (b) (c)

Fig. 4. RSSI vs. Distance plots at different heights a) 6.5ft, b) 3.5ft, c) 1.25ft. RSSI values equal to $-48dBm$ indicate absence of communication between receiver and transmitter

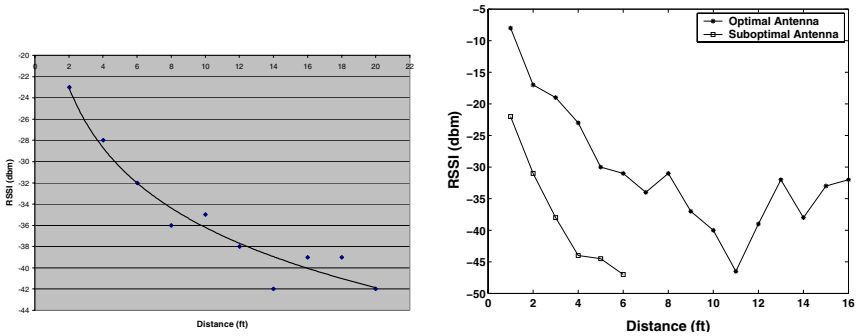

(a) (b)

Fig. 5. a)RSSI vs Distance plots for an obstacle-free environment (basketball court). Each data point is the average RSSI value recorded for 20 packets, b) The effect of using a suboptimal antenna in an obstacle free indoor environment of size $24ft$ x $20ft$.

ability distribution we can map an RSSI value to a specific distance with a given probability. The higher the probability the higher the accuracy of the distance estimation.

Figures 4a, 4b, and 4c clearly show that different antenna orientations can produce different sets of RSSI values for the same distances between receiver and transmitter. In practice, this implies that the raw RSSI values cannot be directly translated to distance information. Extra knowledge about the specific antenna orientation that corresponds to this set of RSSI values is needed. Furthermore, our results show that even if we are able to map a set of RSSI values to a specific antenna orientation this does not necessarily mean that we can extract any useful distance information. The reason is that some antenna orientations do not provide a consistent signal attenuation.

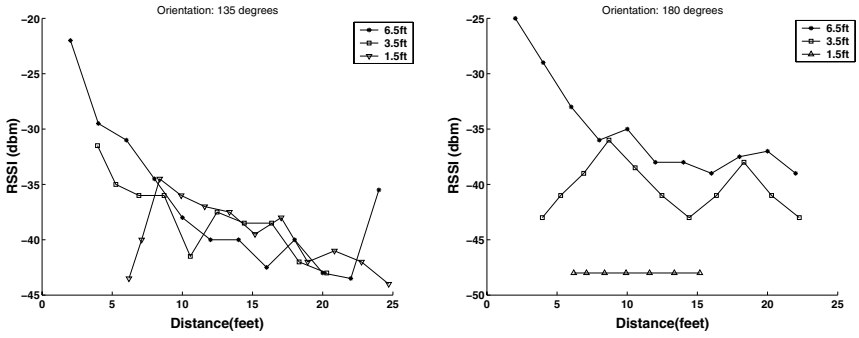

(a) (b)

Fig. 6. a) The best angle between receiver and transmitter, b) One of the worst angles between the receiver and the transmitter. RSSI values equal to $-48dBm$ indicate absence of communication between receiver and transmitter.

Figures 6a and 6b provide some more insight to the antenna orientation effect. Figure 6 shows the best transmitter antenna orientation. Note that a single signal propagation model can be extracted that is independent of the height of the receiver.

On the other hand, Figure 6a shows the worst transmitter antenna orientation. It is obvious that any attempt to infer distance information directly from the RSSI values is impossible. Different heights of the receiver produce very different RSSI values. However, when the receiver is at $6.5ft$ height a signal propagation model can still be extracted. This implies that when the receiver is at $6.5ft$ the radiation pattern of the antenna seems to be very symmetric. This allows us to infer a signal propagation model independently of the antenna orientation of the transmitter. In other words, when the height difference between the transmitter and the receiver is small, antenna orientation does not affect the signal propagation model. But, as figure 6b shows, when the height difference between the transmitter and the receiver increases then the antenna orientation becomes a major factor that greatly affects the signal propagation model.

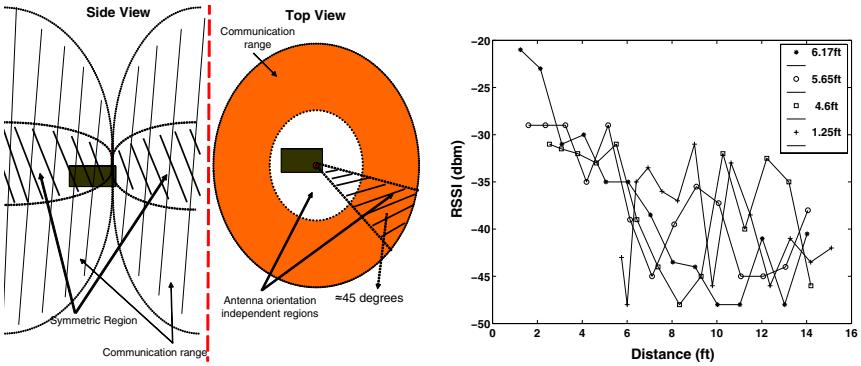

Fig. 7. a) Radiation Pattern of the monopole antenna, b) Indoors antenna characterization. RSSI values equal to $-48dBm$ indicate absence of communication between receiver and transmitter.

This can be seen in figure 7 where the radiation pattern of our monopole antenna is shown. The radiation pattern was constructed using all the measurements we collected in the basketball court. The shaded region of the antenna radiation pattern is the symmetric region for which a single signal propagation model can be extracted. Since the antenna orientation is not a major factor when the receiver and the transmitter are at the same height, the log-normal shadowing model is very accurate in the case of a 2-D sensor network deployment at an obstacle-free environment (outdoor deployment). However, the log-normal shadowing model is not able to capture the effect of the transmitter's antenna orientation in the case of a 3-D sensor network deployment even in an obstacle-free environment.

Consequently, a robust RSSI localization method should try to operate only in the shaded region of the antenna radiation pattern ,shown in Figure 7, where the log-normal shadowing model seems to hold. This requires isolating the shaded area from the rest of the communication region where the RSSI values are significantly affected by the antenna orientation of the transmitter and they cannot provide any reliable distance or location information. To demonstrate the difficulty of this task, consider the following case where a beacon is transmitting packets and a set of receivers listen the packets and record the RSSI values which are then send back to the beacon node. The beacon node is aware of a set of pairs of the following format: $< nodeID, RSSI >$. How can the beacon identify the nodes that were in the shaded area of its communication range? The only case where the beacon is able to identify those nodes is the case where the RSSI values recorded on the nodes that were in the shaded area of the communication range of the beacon node are unique. In other words, there is a unique set of RSSI values that can be recorded on the receiver only when the receiver is in the symmetric region of the communication range of the transmitter. Unfortunately, Figures 4 and 6 show that this unique set of RSSI values is very small and covers only a small range of short distances.

6.3 Antenna Orientation in Indoor Environments

In this section we focus on the effect of the indoor environment on the received signal strength between a pair of communicating nodes. Our first indoors experiment focused on the effect of reflections on the antenna radiation pattern. We tried to replicate the experiment that we run in the basketball court in the 3-D testbed $(15ft(W) \times 20ft(L) \times 10ft(H))$ that is installed in our lab. Exactly the same transmitter that was used in the basketball court experiment was placed at a height of approximately $7ft$ from the ground. The same receiver that was used in the basketball court experiment was placed in four different heights from the ground: $1.25ft$, $4.6ft$, $5.65ft$, and $6.17ft$. For each one of these heights the receiver recorded the RSSI values for different distances from the transmitter with a distance resolution of $1ft$(the transmitter was transmitting packets at the same power level as in the basketball court, $-15dBm$). In this experiment we focused only on a single transmitter antenna orientation, the one that gave us a single signal propagation model that was independent of the height of the receiver(Figure 6) in the obstacle-free environment.

The RSSI values that were recorded on the receiver for all the different distances and for all the different heights of the receiver can be seen in Figure 7b. When the receiver is at $6.17ft$ from the ground a clear log-normal signal propagation model can be derived as in the case of the obstacle-free environment. However, for the other three heights of the receiver the RSSI values seem totally random and no actual distance information can be extracted from these sets of RSSI values. What is even more interesting, is the fact that the randomness that the reflections introduce in the RSSI values directly affects the symmetric region of the antenna and makes it significantly narrower. Note that every RSSI value that is equal or smaller than $-30dBm$ can actually correspond to any distance

that is larger than $1.6ft$ and smaller than the communication range. The only RSSI values that can be used to accurately estimate the distance between the nodes are the RSSI values that are higher than $-30dBm$. This range of RSSI values can only be produced by the symmetric region of the antenna and it is not affected by the reflections in the room or the height of the receiver. In addition, this range of RSSI values can be fitted to a linear signal propagation model and not to a log-normal signal propagation model. Unfortunately, the maximum distance that this region of RSSI values can cover is very small and approximately $3ft$ to $4ft$. This suggests that even for small rooms a very large number of sensor nodes is required in order to perform accurate RSSI localization.

6.4 Indoor Testbed Experiment

In order to verify the results of the previous section, we deployed 38[1] nodes with 2.9inch antennas on our 3-D testbed located inside our lab. The nodes were placed in 3-dimensions inside the testbed as shown in Figure 1b. The antennas of all the nodes on the floor were pointing to the ceiling and the antennas of the nodes on the testbed were pointing either towards the center of the testbed or towards the floor. In all cases, the antennas were vertical with respect to the PCB of the XYZ sensor node.

In our experiment, each node broadcasts 10 packets at each one of the eight available power levels. All the nodes that hear a packet record the RSSI value for this packet and the sender id. At every time instant only one node is broadcasting packets. After a node has finished transmitting packets, a gateway node connected to a PC polls the recorded data from each node in the testbed separately. This process continues until all nodes transmit 10 packets at each power level. The experiment took place during the night when no people were in the lab.

Received Signal Strength Data. Figures 8a, 8b, 8c show the recorded RSSI values versus the true distances that they correspond to for different power levels and for all 38 nodes. It is obvious that no actual distance information can be extracted directly from the RSSI values. This is due to the reflections and the random placement of the nodes which created communicating pairs of nodes with random pairwise antenna orientations. Note, that as the transmitting power level used decreases, the RSSI data starts looking less random. The reason is that as the power level increases the reflections in the testbed also increase. However, even at the low power level it is very difficult to fit the RSSI data to a signal propagation model.

Connectivity and Link Symmetry. Our 38 node deployment also provided useful insight about the connectivity and the symmetry of the links in a real IEEE 802.15.4 sensor network. Figures 10a, 10b, and 10c show the connectivity achieved by the lowest, low and maximum power levels respectively.

[1] Initially we deployed 40 nodes. Unfortunately, as it can be seen in Figure 10, the batteries of nodes 20 and 21 were not full and therefore these nodes did not send/receive any packets.

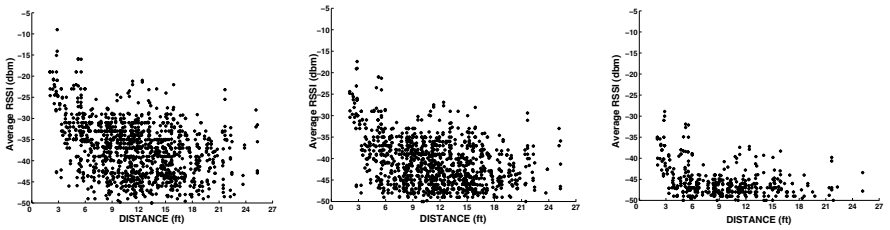

(a) (b) (c)

Fig. 8. RSSI vs Distance plots for the 38 node indoor sensor network deployment at different power levels: a) 0dBm, b) -5dBm, c) -15dBm

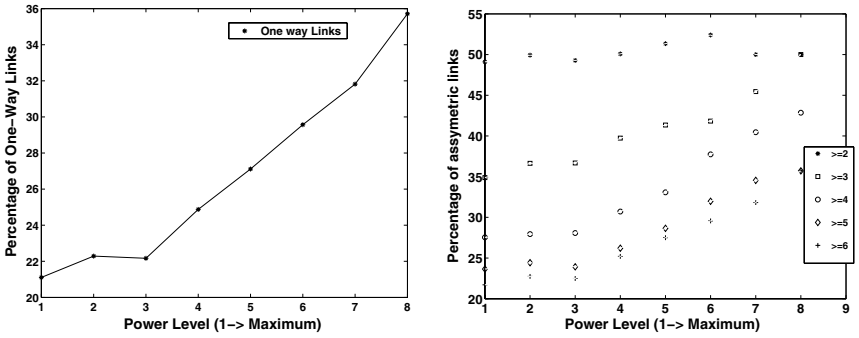

(a) (b)

Fig. 9. Percentage of a) One-way links and b) asymmetric links

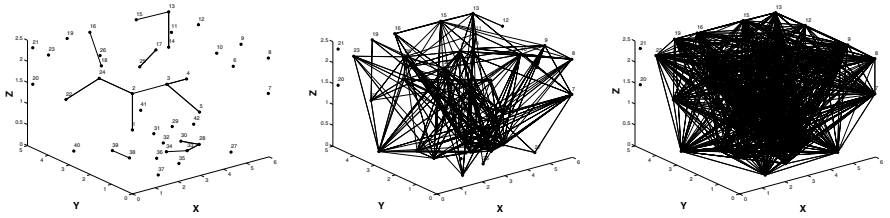

(a) (b) (c)

Fig. 10. Connectivity plots for the 38 node indoor sensor network a)-25dBm b) -15dBm, c) 0dBm. Nodes 20 and 21 were not equipped with fully charged batteries.

Figures 9a and 9b show the percentage of one-way links and the percentage of asymmetric[2] links respectively. As the power level of transmission decreases

[2] We call (A, B) link an asymmetric link if the RSSI value recorded at B when A is transmitting is different than the RSSI value recorded at A when B is transmitting. We call (A, B) link an one-way link if node A can reach node B but node B cannot reach node A. Asymmetric links include the one-way links.

the percentage of asymmetric links and their absolute difference as well as the percentage of one-way links increase. What is even more important, is the fact that the asymmetry of the links does not depend on the actual RSSI values. Our experimental data show that when node A transmits packets, node B might record a very high RSSI value that can be even equal to $-23dBm$ or -25dBm. However, when node B transmits packets, node A might record a very small RSSI value or it might not record any RSSI value at all because it is not able to receive any packets. Our experimental results, shown in Figure 9, show that the percentage of asymmetric links vary from 21% to 36% of the total number of links in the network depending on the power level used during transmission.

7 Discussion

Based on our detailed characterization we found that antenna orientation greatly impacts RSSI and link asymmetry in indoor and outdoor scenarios. This is especially the case in 3-D indoor deployments with random antenna orientations. These observations influence the assumptions of many node localization algorithms that utilize RSSI information. This includes RSSI distance prediction and profiling algorithms as well as other statistical approaches. Our results show that direct distance prediction from raw RSSI data in 3-D indoor environments is impossible. For profiling approaches, our measurements show that antenna orientation information should be included in the fingerprint. However, even if the antenna orientation that corresponds to a set of RSSI values is known it might be impossible to infer any distance information since some antenna orientations do not provide a consistent signal attenuation. This observation shows that modeling the antenna orientation effect as a random variable with gaussian distribution, as it is modeled in equation 1, is not realistic.

Our experiments also show that the antenna orientation has a great impact on the ordering of the RSSI values. The ordering of RSSI values is meaningful only when the communication takes place in the symmetric region of the antenna as it is shown in Figure 7(a). According to our findings this region of the antenna is only a small fraction of the communication range and therefore the ranking of the RSSI values provides little or no information in the case of 3-D deployments where the antenna orientations of the communicating nodes are almost random.

The antenna orientation effect has also implications on the statistical RSSI localization algorithms. In most probabilistic algorithms a probability distribution, usually gaussian, of the RSSI values is assumed. In general, such an assumption holds only in the symmetric region of the antenna. When the communication between two nodes takes place in the non-symmetric region of the antenna, which is generally the case in a 3-D network deployment, the variation in the RSSI values cannot be modeled by a gaussian distribution since, according to our experiments, there is a huge variation in the RSSI values. Consequently, our observations suggest that new probabilistic models that better capture RSSI variations need to be developed for 3-D environments.

In the case of indoor environments, reflections become the main problem in performing RSSI distance prediction. Only a very small range of RSSI values can be used for extracting distance information for up to $3-4ft$. In this region, RSSI changes linearly with distance. In addition, our findings show that 3-D indoor sensor network deployments suffer of a high degree of link asymmetry. This link asymmetry is due to the multipath and fading effects as well as due to the random pairwise antenna orientations used during communication.

8 Conclusions

We have conducted an empirical study of signal strength behavior using monopole antennas and the widely used Chipcon CC2420 radio. Our experiments in a large open space with minimal multipath effects have shown that antenna orientation corrupts signal strength. This significantly alters the quality of information that RSSI can provide for deriving spatial relationships. Our results and experience from this work show that signal strength localization will work in specially instrumented scenarios. In other scenarios and $3D$ deployments, signal strength localization remains an extremely challenging task. Statistical techniques and specific deployment scenarios will mitigate some of these challenges. However, the large amount of characterization needed will make the use of signal strength approaches with low power radios practically impossible. Our study also provides valuable insight into link asymmetry in indoor $3D$ deployments.

Acknowledgment

This work was supported in part by the National Science Foundation under award #0448082 and a gift from OKI Semiconductors. The authors would also like to thank Prof. Sekhar Tatikonda for his valuable feedback on this work.

References

1. P. Bahl and V. N. Padmanabhan. RADAR: An in-building RF-based user location and tracking system. In *Proc. IEEE Infocom*, pages 775–784, Tel-Aviv, Israel, April 2000.
2. M. Berna, B. Lisien, B. Sellner, G. Gordon, F. Pfenning, and S. Thrun. A learning algorithm for localizing people based on wireless signal strength that uses labeled and unlabeled data. In *Proceedings of IJCAI 03, pages 1427-1428*, 2003.
3. P. Castro, P. Chiu, T. Kremenek, and R. Muntz. A Probabilistic Location Service for Wireless Network Environments. *Ubiquitous Computing 2001*, September 2001.
4. Chipcon: CC2420 802.15.4 compliant radio. http://www.chipcon.com.
5. D.Niculescu and B. Nath. Vor base stations for indoor 802.11 positioning. In *Proceedings of Mobicom*, 2004.
6. E. Elnahrawy, X. Li, and R. M. Martin. The limits of localization using signal strength: A comparative study. In *Proceedings of Sensor and Ad-Hoc Communications and Networks Conference (SECON), Santa Clara California*, October 2004.

7. T. He, C. Huang, B. Blum, J. Stankovic, and T. Abdelzaher. Range-free localization schemes for large scale sensor networks. In *International Conference on Mobile Computing and Networking(Mobicom), September 14-19 San Diego California*, September 2003.
8. Jeffrey Hightower, Roy Want, and Gaetano Borriello. SpotON: An indoor 3d location sensing technology based on RF signal strength. UW CSE 00-02-02, University of Washington, Department of Computer Science and Engineering, Seattle, WA, February 2000.
9. Konrad Lorincz and Matt Welsh. Motetrack: A robust, decentralized aproachto rf-based location tracking. In *Proceedings of the International Workshop on Location- and Context-Awareness (Loca 2005)*, 2005.
10. D. Lymberopoulos and A. Savvides. Xyz: A motion-enabled, power aware sensor node platform for distributed sensor network applications. In *IPSN, SPOTS track*, April 2005.
11. D. Madigan, E. Elnahrawy, and R. Martin. Bayesian indoor positioning systems. In *Proceedings of INFOCOM 2005, Miami, Florida*, March 2005.
12. D. Niculescu and B. Nath. Localized positioning in ad hoc networks. In *Proceedings of the First IEEE International Workshop on Sensor Network Protocols and Applications*, San Diego, CA, May 2003.
13. N. Patwari and A. O. Hero III. Using proximity and quantized rss for sensor localization in wireless networks. In *WSNA03*, San Diego, CA, September 2003.
14. Prasithsangaree, P. Krishnamurthy, and P. K. Chrysanthis. On indoor position location with wireless lans. In *The 13th IEEE International Symposium on Personal, Indoor, and Mobile Radio Communications (PIMRC 2002)*, 2002.
15. S. Ray, W. Lai, and I. Pascalidis. Deployment optimization of sensornet-based stochastic location-detection systems. In *Proceedings of INFOCOM 2005, Miami, Florida*, March 2005.
16. S. Saha, K. Chaudhuri, D. Sanghi, and P. Bhagwat. Location determination of a mobile device using ieee 802.11 access point signals. In *IEEE Wireless Communications and Networking Conference (WCNC)*, 2003.
17. Scott Y. Seidel and Theodore S. Rapport. 914 MHz path loss prediction model for indoor wireless communications in multifloored buildings. *IEEE Transactions on Antennas and Propagation*, 40(2):207–217, February 1992.
18. R. Stoleru and J. Stankovic. Probability grid: A location estimation scheme for wireless sensor networks. In *Proceedings of Sensor and Ad-Hoc Communications and Networks Conference (SECON), Santa Clara California*, October 4-7 2004.
19. P. Myllymaki T. Roos and H. Tirri. A statistical modeling approach to location estimation. In *IEEE Trnsactions on Mobile Computing*, pages 1:59–69, 2002.
20. K. Whitehouse, A. Woo, C. Karlof, and D. Culler F. Jiang. The effects of ranging noise on multi-hop localization: An empirical study. In *Proceedings of Information Processing in Sensor Networks (IPSN), Los Angeles, CA*, April 2005.
21. K. Yedavalli, B. Krishnamachari, S. Ravula, and B. Srinivasan. Ecolocation: A technique for rf based localization in wireless sensor networks. In *Proceedings of Information Processing in Sensor Networks (IPSN), Los Angeles, CA*, April 2005.